DOI: 10.1002/ange.201002430

Dimpled Gold Nanoplates

Morphosynthesis of Nanostructured Gold Crystals by Utilizing Interstices in Periodically Arranged Silica Nanoparticles as a Flexible Reaction Field**

*Yoshiyuki Kuroda and Kazuyuki Kuroda**

Nanostructural and morphological design of gold has attracted great attention because of its chemical stability, high conductivity, and quantum-size effects. Nanostructured gold materials with various morphologies[1] show unique optical properties due to their localized surface plasmon resonance[2] and catalytic activity.[3] Ordered arrays of nanostructured gold with various arrangements that depend on their morphology are also important for the fabrication of hierarchically organized functional materials.[4] However, the applications of nanostructured gold are often limited because of its tendency to form unstable aggregates. To circumvent this problem, the formation of three-dimensionally extended frameworks is quite effective. Such three-dimensionally nanostructured gold materials are stable to catalytic reactions[5] and promising for various applications, such as electrochemistry, sensing, and surface-enhanced Raman scattering.[5–7]

However, the design of highly ordered three-dimensional gold nanostructures is quite limited because of the difficulty of controlling the growth of gold. Three-dimensional mesoporous gold materials are formed by a dealloying technique, whereas their nanostructures are not ordered.[5] Though various mesoporous metals have been prepared by soft and hard templating techniques,[8] the nanostructured gold materials prepared by using nanoscale hard templates have been limited to nanoparticles and nanowires without specific three-dimensional nanostructures.[9] Colloidal templating is one of the most useful techniques to form three-dimensionally ordered macroporous materials.[10] By replicating periodically arranged silica nanoparticles with relatively small diameter,[11] three-dimensionally ordered mesoporous (3DOM) materials, such as polymers,[12] carbon,[11a] and platinum,[13,14] have been prepared. Studies on silica nanoparticles assembled into thin films,[15a] patterned structures,[15b] and one-dimensional arrays[15c] have also been reported. Although macroporous gold with submicrometer-scale periodicity is formed by using large templates,[6] disordered mesoporous gold is formed when small silica nanoparticles (ca. 50 nm) are used as templates.[13] The rapid growth of gold may cause collapse of the three-dimensional structure of templates due to the structural mismatch between templates and gold.

To achieve slower crystal growth, we have focused on vapor infiltration of a reducing agent (dimethylamine–borane, DMAB) to deposit gold inside the template (denoted vapor reduction). We have applied this technique for the formation of mesoporous platinum by replicating lyotropic liquid-crystalline templates[16] or colloidal crystal templates.[14] It allows both a slower reduction rate and lower reaction temperature than reduction with H_2.[13]

To our surprise, during the course of this study, many gold particles deposited in the interstices of periodically arranged silica nanoparticles by vapor reduction showed a two-dimensional morphology in spite of the three-dimensional interstitial nanospaces of the template. It can be explained by the interstices in the template acting as a flexible reaction field to relax the strain due to structural mismatch between template and gold, which is analogous to morphosynthesis[17] utilizing reaction fields provided by gel matrices[18] and liquid crystals.[19] A single nanoparticle acts as a rigid template on the microscopic scale, while on the macroscopic scale periodically arranged nanoparticles can alter their interstitial nanospaces, as layered crystals accommodate guest species by changing their interlayer spaces.[20] Furthermore, the reduction process was found to be critical to the morphological and nanostructural variation of gold (Scheme 1). We investigated another method by mixing DMAB and the composite containing the template and $HAuCl_4$ in the solid state to alter the reduction kinetics (denoted solid reduction); 3DOM gold with pore size much smaller than those reported previously for macroporous gold[6] was then formed. Thus, the nanoparticle assemblies are found to be more useful scaffolds both for templating and morphosynthesis than previously expected. This concept using a silica nanoparticle

[*] Y. Kuroda, Prof. Dr. K. Kuroda
Department of Applied Chemistry, Faculty of Science & Engineering, Waseda University
Ohkubo 3-4-1, Shinjuku-ku, Tokyo 169-8555 (Japan)
Fax: (+81) 3-5286-3199
E-mail: kuroda@waseda.jp
Homepage: http://www.waseda.jp/sem-kuroda_lab/
Prof. Dr. K. Kuroda
Kagami Memorial Research Institute for Materials Science and Technology, Waseda University
Nishi-waseda 2-8-26, Shinjuku-ku, Tokyo 169-0051 (Japan)

[**] The authors are grateful to Prof. Osamu Terasaki (Stockholm University), Prof. Lennart Bergström (Stockholm University), Dr. Yasuhiro Sakamoto (Osaka Prefecture University), and Dr. Yusuke Yamauchi (National Institute for Materials Science, Tsukuba) for their fruitful discussion. This work was supported by the Elements Science and Technology Project and the Global COE program "Practical Chemical Wisdom" from MEXT (Japan). The A3 Foresight Program "Synthesis and Structural Resolution of Novel Mesoporous Materials" supported by the Japan Society for Promotion of Science (JSPS) is also acknowledged. Y.K. is grateful for financial support via a Grant-in-Aid for JSPS Fellows from MEXT.

Supporting information for this article is available on the WWW under http://dx.doi.org/10.1002/anie.201002430.

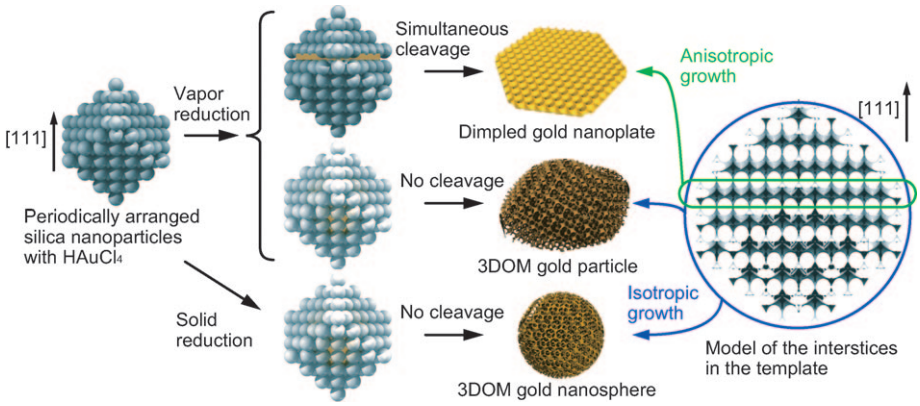

Scheme 1. Proposed pathways to form nanostructured gold materials.

assembly as a flexible matrix is promising for the design of hierarchically nanostructured materials that are effective for the control of materials properties on different length scales.

Vapor reduction of $HAuCl_4$ in the template provides unique two-dimensional gold crystals with ordered surface nanostructures (denoted dimpled gold nanoplate, Figure 1 a), which is not explained by the general mechanism[10] of colloidal templating. Silica nanoparticles about 40 nm in diameter used as templates were arranged mostly in a face-centered cubic (fcc) lattice (Figure S1 in the Supporting Information), that is, the template can be used for conventional colloidal templating.[10] The high-resolution scanning electron microscopy (HRSEM) image shows dimpled gold nanoplates (Figure 1 a), folded ones (Figure S2 in the Supporting Information), and ill-shaped particles (Figure S3 in the Supporting Information). A small amount of 3DOM gold particles was also observed, and corresponds to the general templating mechanism (Figure 2 a). The X-ray diffraction (XRD) pattern and energy dispersive X-ray (EDX) spectrum show that $HAuCl_4$ was reduced to fcc Au and the template was completely removed (Figures S4 and S5 in the Supporting Information). Therefore, highly ordered gold nanostructures are formed by controlled reduction of $HAuCl_4$ in the interstices. Ill-shaped particles are probably formed outside of the template and in cleaved templates due to diffusion of $HAuCl_4$ during the reduction process. Even though small amounts of 3DOM gold particles and ill-shaped particles were observed, two-dimensional growth in the three-dimensional nanospace was clearly shown, and this is quite a meaningful result for understanding the role of highly ordered nanospaces as reaction fields.

The HRSEM image of dimpled gold nanoplates shows an average lateral size of about 400 nm and a wide size distribution from 90 nm to 2 μm, and they are smaller than the templates (typically >5 μm). The average thickness is about 24 nm with narrow distribution (Figure 1 b). The dimples of about 40 nm in diameter are arranged hexagonally on the surface of the nanoplates. The dimples are located on both the lower and upper sides, which was confirmed by tilting the sample stage (Figure S6 in the Supporting Information). Thus, platelike gold was deposited not on the outer surface but inside the template. This structure cannot be formed by using colloidal monolayers as two-dimensional templates.[21] Such a hexagonal arrangement of dimples corresponding to that of the {111} facet of the template was exclusively observed among the nanoplates ($>90\%$). The few nanoplates showing similar dimples in tetragonal and disordered arrangements correspond to those on the {100} facet and the distorted one. Folded nanoplates show a combination of facets such as {111} and {100}. These results suggest that the nanoplate was formed by aniso-

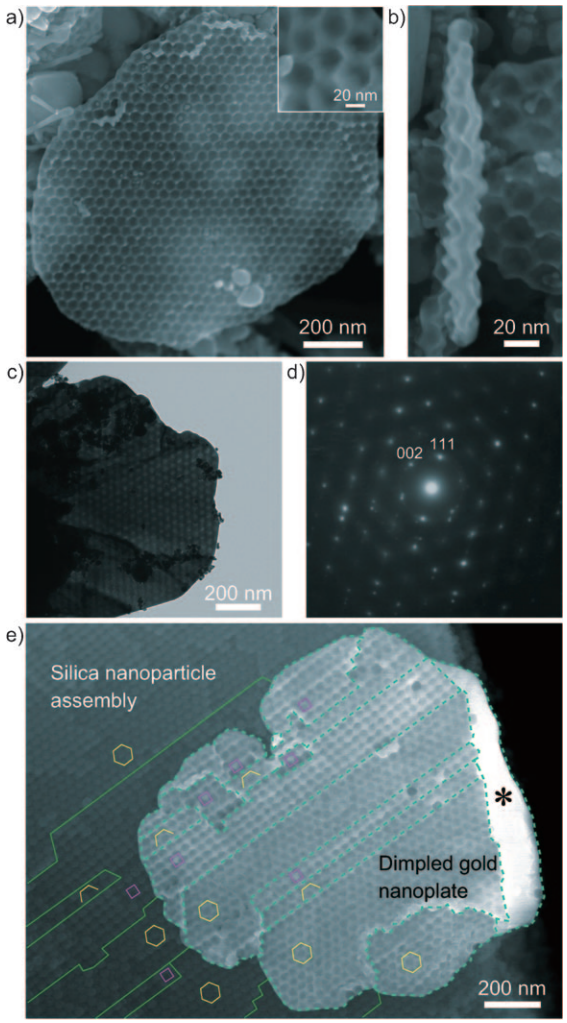

Figure 1. HRSEM images of the dimpled gold nanoplate showing a) the surface and b) the cross section. The inset of a) shows an enlarged image. c) TEM image of the nanoplate and d) its corresponding SAED pattern. e) HRSEM image of the sample before removal of the template. The various facets of the silica nanoparticle assembly and the parts with various arrangements of dimples are outlined by solid and dotted lines, respectively. The hexagons, squares, and asterisk indicate the arrangements attributable to {111}, {100}, and unstructured regions, respectively.

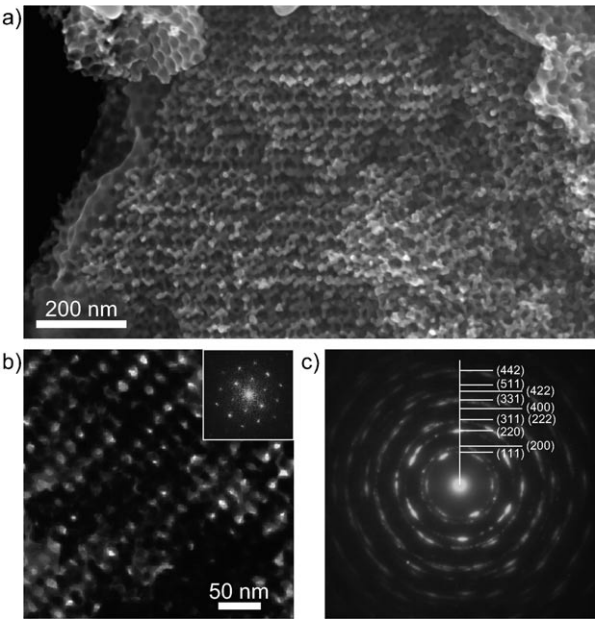

Figure 2. a) HRSEM image of the 3DOM gold particle prepared by vapor reduction. b) TEM image of the 3DOM gold particles and corresponding Fourier transform (inset). c) SAED pattern taken at the same area as b).

tropic growth of gold in a specific crystallographic plane of the silica nanoparticle assembly.

The crystalline domain size and its orientation were characterized by transmission electron microscopy (TEM). The selected-area electron diffraction (SAED) pattern of a single nanoplate (Figure 1c) shows intense spots attributable to single-crystalline fcc Au along the $[\bar{1}10]$ zone axis (Figure 1d). Most of the other nanoplates are also single crystals. Some of them, though far fewer, consist of a few domains whose size is in the submicrometer range (Figure S7 in the Supporting Information). These results show that the number of nuclei is quite small. It is quite rare that a highly ordered nanostructure is formed with retention of such a large single-crystalline domain. The structure may be effective for forming catalytically active high-index facets and improving the conductivity, optical property, and mechanical strength. According to the literature,[1] gold nanorods or nanoplates show specific crystalline orientations, which are formed by preferential growth of specific facets due to the effects of surface stabilizers or stacking faults. The dimpled gold nanoplate in the present study shows no obvious crystalline orientation, and therefore the formation of dimpled gold nanoplate is not explained by such a preferential growth.

The anisotropic growth of gold in a specific plane of the silica nanoparticle assembly can be explained by partial cleavage of the assembly. Continuous growth of gold among the silica nanoparticles probably causes strain in the assembly, which is probably simultaneously cleaved to release the strain. Gold grows through the two-dimensional nanospace formed by cleavage, and dimples are formed on the surfaces by replication of the cleaved surfaces of the template. Because the density of siloxane bonds among silica nanoparticles is quite low, it is reasonable that cleavage occurs under strong strain. The HRSEM image of the sample before removal of template (Figure 1e) gives evidence that the assembly was cleaved during growth. The image shows the dimpled gold nanoplate on the cleaved surface of the assembly, which is also schematically explained in Figure S8a in the Supporting Information. The presence of the dimples on the upper side of the nanoplate shows that part of assembly was evidently delaminated after crystal growth. The cleaved tent-shaped surface of the template exposes the {111} and {100} facets, and this results in formation of a folded nanoplate. The possibility that the observed nanoplate was formed in another template and moved to the present position is quite low, because the {111} and {100} facets of the template are consistent with the arrangements of the dimples on the gold nanoplate. The stereoscopic anaglyph version of the image (Figure S9 in the Supporting Information) shows that the morphology of the folded nanoplate is well consistent with the surface relief of the template. Furthermore, no windows were observed on the surface of the dimples (Figure 1a, inset), which means that the silica nanoparticles are disconnected where gold is deposited. Windows are always formed where silica nanoparticles are connected. The assembly probably contains defects,[22] which may affect the direction of cleavage propagation to form tent-shaped cleaved surfaces. The formation of folded nanoplates shows that lateral crystal growth occurs even between such tent-shaped cleaved surfaces. A similar HRSEM image with the unfolded nanoplate is also shown in Figure S8b in the Supporting Information. Because 3DOM gold was formed by using the same template under different reduction conditions, it is clear that the nanoplate was formed not in an initially formed cleavage before deposition but in a simultaneously formed cleavage during growth.

The ordering of nanoparticles in the template is essential to the formation of the dimpled gold nanoplate. When a disordered assembly was used as template, disordered networks of gold without platelike morphology were observed (Figure S10 in the Supporting Information). Therefore, the anisotropic crystal growth of gold is probably governed by the cooperative transformation of the ordered arrangement of the nanoparticles. Disassembly of three-dimensional nanostructures to form unique cubic nanoparticles has been reported,[23] whereas the mechanism is not related to the long-range ordering reported here.

The preferential formation of hexagonally arranged dimples is probably due to the preference for cleavage along the {111} plane of the template, because the {111} facet is the most stable facet with a two-dimensional close-packed structure in the template.

In the case of fcc metals, the most stable facet is calculated to be the {111} facet.[24] Once cleavage occurs along a specific direction, gold probably grows along the same direction because diffusion between the cleaved surfaces is faster than among the closely packed silica nanoparticles.

In our previous report,[14] only 3DOM platinum was obtained as major product by almost the same process. We suppose that rapid crystal growth of gold due to fast reduction of $HAuCl_4$ should cause much strain in the template. The reduction of $HAuCl_4$ in the template was completed in about

one day, which is much faster than that of H_2PtCl_6, which takes about three days.

The combination of dimples and two-dimensional morphology is uniquely useful for constructing hierarchical assemblies. Gold nanoparticles can be arranged periodically on the dimples (Figure S11 in the Supporting Information). The distance between the gold nanoparticles is regulated by the dimples, regardless of the size of the gold nanoparticles. Thus, the size, arrangement, and separation of nanoparticles can be controlled independently. The composition of nanoparticles can be extended to other metals, oxides, and semiconductors. The two-dimensional morphology is potentially effective for assembly into thin films and multilayers.[4c,25] The bottom-up fabrication of hierarchical structures is promising for the design of functional materials.[26]

The 3DOM gold particles formed in small amounts by vapor reduction, as described above, are also quite interesting materials because they consist of relatively large crystalline domains. The 3DOM gold particles are up to several micrometers in size (Figure S12 in the Supporting Information). Mesopores about 40 nm in diameter are arranged in an fcc lattice, corresponding to the inverse structure of the periodically arranged silica nanoparticles (Figure S13a in the Supporting Information). The mesopores are interconnected through windows, which suggests no cleavage occurred in the template. The pore walls are not aggregates of nanoparticles like other mesoporous metals.[8] The TEM image and the corresponding Fourier transform show a high degree of nanostructural ordering (Figure 2b and inset). The SAED pattern with intense arcs shows that the product consists of several slightly distorted domains (Figure 2c). This result suggests continuous crystal growth during formation of the 3DOM gold. The somewhat complex SAED pattern is possibly explained by formation of defects in the framework, such as twin planes (Figure S14 in the Supporting Information). The formation of a 3DOM gold is possibly due to locally less concentrated infiltration of $HAuCl_4$.

In contrast, solid reduction of $HAuCl_4$ in the template gives only polycrystalline 3DOM gold nanospheres without ill-shaped particles. The HRSEM images show their spherical morphology (Figure 3a) and highly ordered nanostructure (Figure S13b in the Supporting Information). The TEM image and the ringlike SAED pattern show that the 3DOM gold nanosphere is polycrystalline with smaller domains due to formation of many nuclei (Figure 3b and c). Solid reduction generates multiple nuclei concurrently in many positions in the template, and possibly causes widely distributed smaller strains in the template than vapor reduction. The reduction rate influences the nanostructure of gold because disordered gold similar to that prepared by H_2 reduction[13] is formed when DMAB and the composite containing the template and $HAuCl_4$ are mixed vigorously (Figure S15 in the Supporting Information). The spherical morphology is possibly due to diffusion-limited crystal growth in the three-dimensional interstitial nanospace. Electron transfer by solid reduction is probably much faster than diffusion of $HAuCl_4$ in the template. This result suggests that relatively fast reduction with multiple nucleation is effective to form nanostructures as a single phase without formation of ill-shaped particles, which is quite different from the case of platinum, for which slow crystal growth is better for formation of highly ordered mesoporous materials.[16] When solid reduction was applied for the formation of 3DOM platinum, only platinum nanoparticles about 4 nm in diameter without interconnections were formed (data not shown). This difference should be due to the slow growth of platinum, in which H_2PtCl_6 is completely reduced before formation of the continuous frameworks. This solid reduction method is promising for further nanostructural control of gold by the templating technique. Such a single-phase 3DOM gold nanosphere has never been formed by conventional templating techniques and is potentially useful for catalysts, electrodes, sensors, and optical materials.

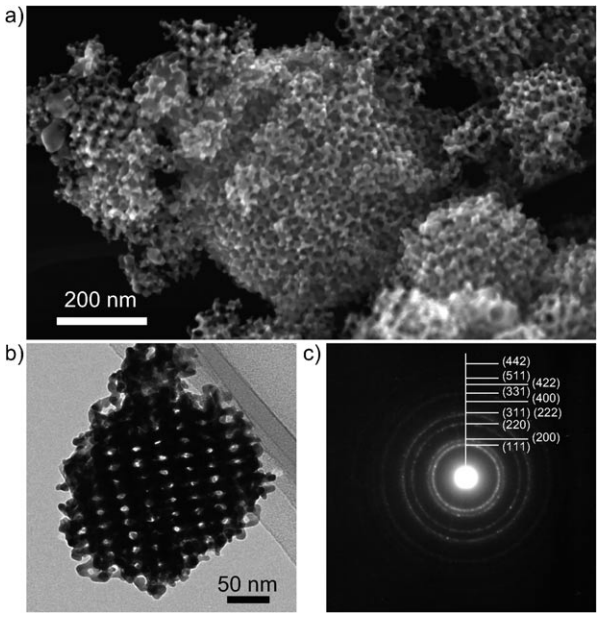

Figure 3. a) HRSEM image of 3DOM gold nanospheres prepared by solid reduction. b) TEM image of the 3DOM gold nanospheres and c) corresponding SAED pattern.

In conclusion, we have demonstrated unique crystal growth of gold in the interstices of periodically arranged silica nanoparticles by controlled crystal growth. The silica nanoparticle assembly acts not only as a rigid template on the microscopic scale but also as a flexible reaction field on the macroscopic scale, like organic matrices. Furthermore, this template has directionality of the interstitial nanospace, whereby gold grows along the fcc {111} plane, which is not achieved by conventional morphosynthesis. The mechanism gives a new insight into the importance of ordered nanostructures. Fast solid reduction with multiple nucleation was specifically effective for obtaining single-phase 3DOM gold nanospheres, which is promising for further applications utilizing the mesoporous structure. The colloidal templating technique is found to be more useful in providing a flexible reaction field for crystal growth than previously expected. Such a dynamic transformation of inorganic nanostructures will be applied for a wide range of materials with compositional, structural, and morphological variations.

Experimental Section

Materials: Tetraethoxysilane (TEOS, Kishida Chemical Co.), and L-lysine (Sigma-Aldrich Co.) were used for the synthesis of the silica nanoparticle assembly. $HAuCl_4{\cdot}4H_2O$ (Kanto Chemical Co., Inc.) was used as a metal source. Dimethylamine–borane (DMAB, Wako Pure Chemical Ind. Ltd.) was used as reducing agent. Hydrofluoric acid (Wako Pure Chemical Ind. Ltd.) and ethanol (Kanto Chemical Co., Inc.) were used for removal of templates.

Synthesis of silica nanoparticle assembly: Silica nanoparticle assemblies were synthesized according to the literature.[11] TEOS and L-lysine were dissolved in deionized water (H_2O:TEOS:L-lysine = 154.4:1:0.02). The mixture was stirred vigorously for 20 h at 60 °C to obtain monodisperse silica nanoparticles ca. 12 nm in diameter. Then, the silica nanoparticles were grown in a mixture containing TEOS and L-lysine to obtain monodisperse silica nanoparticles about 40 nm in diameter. A silica nanoparticle assembly was obtained by drying up the solution and subsequent calcination at 550 °C for 6 h.

Vapor reduction method: The silica nanoparticle assembly was dried under vacuum overnight to remove adsorbed water molecules. An aqueous solution containing 0.4 M $HAuCl_4$ (0.2 mL) was mixed with the silica nanoparticle assembly (1 g). The composite was placed in a closed plastic vessel with DMAB for 1 d at 40 °C according to the reduction technique used for 3DOM platinum.[14] The sample was washed with ethanol and the template was removed by 5% HF aq.

Solid reduction method: The composite including the template and $HAuCl_4$ was gently mixed with solid DMAB, and the mixture immediately turned dark blue. The sample was washed and the template removed by the same method as for vapor reduction.

Characterization: HRSEM images were recorded by a Hitachi S-5500 microscope at an accelerating voltage of 30 kV. TEM images, SAED patterns, and EDX spectra were recorded by a JEOL JEM-2010 microscope at an accelerating voltage of 200 kV. Samples were dispersed in ethanol and mounted on an STEM microgrid for the HRSEM and HRTEM operations. XRD was performed on a Rigaku Ultima-III diffractometer with $Cu_{K\alpha}$ radiation at 40 kV and 40 mA.

Received: April 24, 2010
Revised: June 11, 2010
Published online: August 18, 2010

Keywords: crystal growth · gold · nanoparticles · nanostructures · template synthesis

[1] Y. Xia, Y. Xiong, B. Lim, S. E. Skrabalak, *Angew. Chem.* **2009**, *121*, 62 – 108; *Angew. Chem. Int. Ed.* **2009**, *48*, 60 – 103, and references therein.
[2] S. Link, M. A. El-Sayed, *J. Phys. Chem. B* **1999**, *103*, 8410 – 8426.
[3] M. Haruta, *Gold Bull.* **2004**, *37*, 27 – 36.
[4] a) M. Kanehara, E. Kodzuka, T. Teranishi, *J. Am. Chem. Soc.* **2006**, *128*, 13084 – 13094; b) Q. Liao, C. Mu, D. S. Xu, X. C. Ai, J. N. Yao, J. P. Zhang, *Langmuir* **2009**, *25*, 4708 – 4714; c) N. Malikova, I. Pastoriza-Santos, M. Schierhorn, N. A. Kotov, L. M. Liz-Marzán, *Langmuir* **2002**, *18*, 3694 – 3697.
[5] a) V. Zielasek, B. Jürgens, C. Schulz, J. Biener, M. M. Biener, A. V. Hamza, M. Bäumer, *Angew. Chem.* **2006**, *118*, 8421 – 8425; *Angew. Chem. Int. Ed.* **2006**, *45*, 8241 – 8244; b) A. Wittstock, V. Zielasek, J. Biener, C. M. Friend, M. Bäumer, *Science* **2010**, *327*, 319 – 322.
[6] a) O. D. Velev, P. M. Tessier, A. M. Lenhoff, E. W. Kaler, *Nature* **1999**, *401*, 548; b) R. Szamocki, S. Reculusa, S. Ravaine, P. N. Bartlett, A. Kuhn, R. Hempelmann, *Angew. Chem.* **2006**, *118*, 1340 – 1344; *Angew. Chem. Int. Ed.* **2006**, *45*, 1317 – 1321.
[7] Z. Q. Tian, B. Ren, D. Y. Wu, *J. Phys. Chem. B* **2002**, *106*, 9463 – 9483.
[8] Y. Yamauchi, K. Kuroda, *Chem. Asian J.* **2008**, *3*, 664 – 676, and references therein.
[9] a) C. M. Yang, H. S. Sheu, K. J. Chao, *Adv. Funct. Mater.* **2002**, *12*, 143 – 148; b) A. Fukuoka, H. Araki, Y. Sakamoto, N. Sugimoto, H. Tsukada, Y. Kumai, Y. Akimoto, M. Ichikawa, *Nano Lett.* **2002**, *2*, 793 – 795.
[10] A. Stein, R. C. Schroden, *Curr. Opin. Solid State Mater. Sci.* **2001**, *5*, 553 – 564.
[11] a) T. Yokoi, Y. Sakamoto, O. Terasaki, Y. Kubota, T. Okubo, T. Tatsumi, *J. Am. Chem. Soc.* **2006**, *128*, 13664 – 13665; b) K. D. Hartlen, A. P. T. Athanasopoulos, V. Kitaev, *Langmuir* **2008**, *24*, 1714 – 1720; c) T. Yokoi, J. Wakabayashi, Y. Otsuka, W. Fan, M. Iwama, R. Watanabe, K. Aramaki, A. Shimojima, T. Tatsumi, T. Okubo, *Chem. Mater.* **2009**, *21*, 3719 – 3729.
[12] S. A. Johnson, P. J. Ollivier, T. E. Mallouk, *Science* **1999**, *283*, 963 – 965.
[13] G. L. Egan, J. S. Yu, C. H. Kim, S. J. Lee, R. E. Schaak, T. E. Mallouk, *Adv. Mater.* **2000**, *12*, 1040 – 1042.
[14] Y. Kuroda, Y. Yamauchi, K. Kuroda, *Chem. Commun.* **2010**, *46*, 1827 – 1829.
[15] a) M. A. Snyder, J. A. Lee, T. M. Davis, L. E. Scriven, M. Tsapatsis, *Langmuir* **2007**, *23*, 9924 – 9928; b) Y. Yamauchi, J. Imasu, Y. Kuroda, K. Kuroda, Y. Sakka, *J. Mater. Chem.* **2009**, *19*, 1964 – 1967; c) M. Fukao, A. Sugawara, A. Shimojima, W. Fan, M. A. Arunagirinathan, M. Tsapatsis, T. Okubo, *J. Am. Chem. Soc.* **2009**, *131*, 16344 – 16345.
[16] Y. Yamauchi, A. Takai, M. Komatsu, M. Sawada, T. Ohsuna, K. Kuroda, *Chem. Mater.* **2008**, *20*, 1004 – 1011.
[17] S. Mann, S. L. Burkett, S. A. Davis, C. E. Fowler, N. H. Mendelson, S. D. Sims, D. Walsh, N. T. Whilton, *Chem. Mater.* **1997**, *9*, 2300 – 2310.
[18] Y. N. Tan, J. Y. Lee, D. I. C. Wang, *J. Phys. Chem. C* **2009**, *113*, 10887 – 10895.
[19] T. Kijima, Y. Nagatomo, H. Takemoto, M. Uota, D. Fujikawa, Y. Sekiya, T. Kishishita, M. Shimoda, T. Yoshimura, H. Kawasaki, G. Sakai, *Adv. Funct. Mater.* **2009**, *19*, 545 – 553.
[20] Y. Ide, A. Fukuoka, M. Ogawa, *Chem. Mater.* **2007**, *19*, 964 – 966.
[21] P. Jiang, M. J. McFarland, *J. Am. Chem. Soc.* **2005**, *127*, 3710 – 3711.
[22] R. Rengarajan, D. Mittleman, C. Rich, V. Colvin, *Phys. Rev. E* **2005**, *71*, 016615.
[23] F. Li, Z. Y. Wang, A. Stein, *Angew. Chem.* **2007**, *119*, 1917 – 1920; *Angew. Chem. Int. Ed.* **2007**, *46*, 1885 – 1888.
[24] J. M. Zhang, F. Ma, K. W. Xu, *Appl. Surf. Sci.* **2004**, *229*, 34 – 42.
[25] T. Sasaki, *J. Ceram. Soc. Jpn.* **2007**, *115*, 9 – 16.
[26] a) K. Ariga, Q. M. Ji, J. P. Hill, A. Vinu, *Soft Matter* **2009**, *5*, 3562 – 3571; b) S. A. Claridge, A. W. Castleman, S. N. Khanna, C. B. Murray, A. Sen, P. S. Weiss, *ACS Nano* **2009**, *3*, 244 – 255.

